Genetica (2019) 147:369–379
https://doi.org/10.1007/s10709-019-00077-z

ORIGINAL PAPER

# MITF: an evolutionarily conserved transcription factor in the sea urchin *Paracentrotus lividus*

**Roberta Russo**[1] · **Marco Chiaramonte**[1] · **Nadia Lampiasi**[1] · **Francesca Zito**[1]

Received: 18 June 2019 / Accepted: 9 October 2019 / Published online: 17 October 2019


## Abstract

Microphthalmia-associated transcription factor (MITF) is a member of MYC superfamily, associated with melanocyte cells, as it was discovered in depigmented mice. However, over the last years it was found to be involved in many cellular signaling pathways, among which oncogenesis, osteoclast differentiation, and stress response. In mammals, *Mitf* gene mutations can cause diverse syndromes affecting pigmentation of eyes or skin, bone defects and melanomas. As MITF protein homologs were also found in some invertebrates, we have isolated and characterized the MITF cDNAs from the sea urchin *Paracentrotus lividus*, referred to as *Pl-Mitf*. The in silico study of the secondary and tertiary structure of Pl-Mitf protein showed high conserved regions mostly lying in the DNA binding domain. To understand the degree of evolutionary conservation of MITF, a phylogenetic analysis was performed comparing the Pl-Mitf deduced protein with proteins from different animal species. Moreover, the analysis of temporal and spatial expression pattern of *Pl-Mitf* mRNA showed that it was expressed from the onset of gastrulation of the sea urchin embryo to the pluteus larva, specifically in primary mesenchymes cells (PMCs), the sea urchin skeletogenic cells, and in the forming archenteron, the larval gut precursor. In silico protein–protein interactions analysis was used to understand the association of MITF with other proteins. Our results put in evidence the conservation of the MITF protein among vertebrates and invertebrates and may provide new perspectives on the pathways underlying sea urchin development, even if further functional analyses are needed.

**Keywords** Development · Gene expression · Bioinformatics · Proteins interactions

## Introduction

In all organisms, transcription factors (TFs) are very important key molecules in the complex networks that regulate cell homeostasis/metabolism, signaling pathways and embryogenesis. They have many targets, among which other TFs, able of triggering cascades of events, which serve to lead each cell to play its specific final tasks. TFs are grouped in large families related to the structures of their DNA binding domains, such as the basic Leucine Zipper (bZIP), the Zinc Finger (Znf), the homeodomain Leucine Zipper (HD-Zip), Rel-homology-domain (RHD), the Forkhead box (FOX) and the Helix–Loop–Helix (HLH) (Landschulz et al. 1988; Jones 2004; Katoh and Katoh 2004).

Microphthalmia-associated transcription factor (MITF) is a member of the MYC superfamily, isolated from mice with mutations at the MITF locus associated with defects in pigmentation (Hodgkinson et al. 1993). In addition to defects in pigment cells of the skin, hair and inner ear, MITF controls apoptosis in development and survival of melanocytes, through several target genes, such as Bcl-2, and inhibitors of apoptosis (Lu et al. 2010). In recent years, the function of MITF has been tightly connected to differentiation of malignant melanoma cells (Hartman et al. 2015). However, it has been shown that mutants of this gene also affected several other cell types, such as bone osteoclasts,

Database: Pl-mitf nucleotide sequence data are available in the EMBL databases under the Accession Number: MK229196.

**Electronic supplementary material** The online version of this article (https://doi.org/10.1007/s10709-019-00077-z) contains supplementary material, which is available to authorized users.

✉ Roberta Russo
roberta.russo@irib.cnr.it

✉ Francesca Zito
francesca.zito@irib.cnr.it

[1] Consiglio Nazionale delle Ricerche, Istituto per la Ricerca e l'Innovazione Biomedica, Via Ugo La Malfa 153, 90146 Palermo, Italy

retinal pigment epithelial cells, and mast cells (Jones 2004; Levy et al. 2006). Moreover, a few MITF mutations induce osteoclast defects, which can lead to osteopetrosis (Roundy et al. 2003). It is interesting that just a single site mutation inside the DNA binding region of MITF gene can lead to a malfunctioning protein, and cause a block of its transcriptional activity. In such mutated mice, the bone marrow was compromised and produced a few osteoclasts that were functionally deficient; thus the so called "microphthalmic" animals displayed osteopetrosis similar to animals lacking the Receptor activator of nuclear factor kappa-B ligand (RANKL) (Roundy et al. 2003). In humans, *MITF* mutations cause an auditory-pigmentary Waardenburg syndrome (Widlund and Fisher 2003). The MITF family includes four distinct genes: MITF, TFEB, TFE3, and TFEC (Slade and Pulinilkunnil 2017).

MITF protein is a TF that contains a basic HLH associated with a leucine zipper structure (bHLHzip) at its C-terminal, that binds DNA as homo- or heterodimers. In mammals, there are at least nine isoforms of MITF designated by their unique 5′ ends, i.e. MITF-A, MITF-B, MITF-C, MITF-D, MITF-E, MITF-H, MITF-J, MITF-MC and MITF-M, which show tissue-specific patterns of expression. For example, the isoform E is expressed in osteoclasts, the isoform M is expressed specifically in melanocytes, and the isoform MC is expressed selectively in mast cells (Levy et al. 2006; Hartman et al. 2015).

MITF protein binds to M-boxes (5′-TCATGTG-3′) and symmetrical DNA sequences (Ephrussi-boxes) (5′-CAC GTG-3′) present in the promoters of target genes, such as Bcl2, Tyrosinase, Tyrp1 (Slade and Pulinilkunnil 2017).

In invertebrates, MITF orthologs have been identified in the nematode *Caenorhabditis elegans* (Rehli et al. 1999), in ascidia (Yajima et al. 2003) and very recently in mollusks (Mao et al. 2019). In *Drosophila melanogaster*, MITF gene is expressed in the eye imaginal disc during embryogenesis (Hallsson and Benedikta 2007).

The availability of the *Strongylocentrotus purpuratus* sea urchin annotated genome (Sodergren et al. 2006) has allowed the systematic identification of all TFs families (Howard-Ashby et al. 2006a; Materna et al. 2006; Rizzo et al. 2006; Tu et al. 2006). In *S. purpuratus*, one *Mitf* gene is annotated, *Sp-Mitf* (SPU_008175) (Howard-Ashby et al. 2006b), and three isoforms differing in their amino acids at the 5′ end are present in the Genbank.

Sea urchin occupies an important phylogenetic position, being a deuterostome like the vertebrates, and thus representing a strong evolutionary link between invertebrates and vertebrates. In addition, embryos and immune cells of the mediterranean sea urchin *Paracentrotus lividus* have been used as sentinels of environmental stress for many years, and are valid tools for discovering molecular and regulatory pathways (Bonaventura et al. 2018; Chiaramonte 2019; Ragusa et al. 2019). Thus, the sea urchin *P. lividus* can be considered as an interesting model for studying the role of TFs that are common to many organisms and an ethical and validated alternative to the use of higher class of animals.

Here, we report for the first time the isolation of a member of the MITF bHLHzip family from *P. lividus* sea urchin, referred to as *Pl-Mitf*, and the characterization of its cDNAs. We describe the phylogenetic relationship among Pl-Mitf protein and MITF proteins from other invertebrate and vertebrate organisms. We then determined the temporal and spatial expression profile of *Pl-Mitf* mRNA during *P. lividus* embryo development and performed MITF protein–protein interactions analysis.

## Materials and methods

### Sampling of animals

Gametes were collected from adult sea urchin *P. lividus,* fished in the North-Western coast of Sicily of Mediterranean Sea. Eggs were fertilized and embryos were grown in Millipore (Billerica, MA, USA, 0.22 µm) filtered sea water (MFSW) containing antibiotics (50 mg/1 streptomycin sulfate and 30 mg/1 penicillin), at the dilution of 4.000 embryos/ml and at the temperature of 18 ± 1 °C.

### RNA extraction, cDNA synthesis, cloning and sequencing

Total RNA from gastrula embryos was extracted using "GenElute Mammalian Total RNA Miniprep Kit" according to the manufacturer's instructions (Sigma Chemical Co., St Louis, MO, USA) and quantified using a bio-photometer (Eppendorf S.r.l., Hamburg, Germany). Before synthesizing cDNA, we tested the obtained RNAs by PCR with primers for the *Pl-Z12-1* reference gene to ensure no genomic contamination. Total RNAs (1 µg) were reverse transcribed according to the manufacturer's instructions (Applied Biosystems, Life technologies, Carlsbad, CA, USA). An aliquot of the synthesized cDNA (20 ng) was used to perform the polymerase chain reaction (PCR). The amplicons obtained from the PCR reaction were cloned in the pGEM-Teasy vector, following the Promega manufacturer instruction manual (Promega, Madison, WI, USA) and sequenced by a service company (BIO-FAB research srl, Rome). The isolated sequence has been deposited at NCBI (http://www.ncbi.nlm.nih.gov/) under the following accession number MK229196.

### Quantitative polymerase chain reaction (QPCR)

Quantification of gene expression was performed by using the StepOnePlus real-time PCR, as described in the

manufacturer's manual (Applied Biosystems) with a Comparative Threshold Cycle Method using SYBR Green chemistry (Livak and Schmittgen 2001). The *Pl*-Z12-1 mRNA was used as the internal endogenous reference gene (Costa et al. 2012). The QPCR was run as follows: 1× cycle denaturing 95 °C for 10′ for DNA polymerase activation; 38× cycles: melting 95 °C for 15″, annealing/extension 60 °C for 60″. *Pl-Mitf* used primers were: Forward: 5′TGATCC CGACCAGCGACAGAACA3′; Reverse: 5′TCTAATTGT CTCTGTCTACCCTCA 3′. The amplicon lenght was 120 nt, located in the middle of the gene.

## Statistical analysis

Statistical analysis was performed on QPCR values obtained from at least three independent experiments using the one-way ANOVA analysis of variance test followed by Tukey's multiple comparison test, using R statistical software (http://www.r-project.org). The significance of the results obtained was assessed through the Student's *t* test, with considered significance at $p < 0.05$.

## In silico analysis of the protein and phylogenetics

The deduced protein of Pl-Mitf and the proteins interactions (STRING analysis) were performed using the ExPASy proteomic server tools (http://www.expasy.org/). Homologues of the proteins from different organisms, belonging to both invertebrate and vertebrate phyla, have been obtained by the BLAST program (Basic Local Alignment Search Tool) (http://blast.ncbi.nlm.nih.gov/) and their Accession numbers are indicated in Table 1. Multiple alignments of the obtained proteins were performed by Clustal Omega (http://www.ebi.ac.uk/Tools/msa/clustalo/). Evolutionary analysis was conducted in MEGA6 (Tamura et al. 2013), using the Neighbor-Joining (NJ) method (Saitou and Nei 1987). The evolutionary distances were computed using the Poisson correction method (Zuckerkandl and Pauling 1965). Predictions of Secondary structure models of Pl-Mitf protein were obtained by Phyre2 bioinformatic tool (Kelley and Sternberg 2009). The tertiary structure of Pl-Mitf protein was found by using the software I-Tasser (https://zhanglab.ccmb.med.umich.edu/I-TASSER). The software Netphos 3.1 (http://www.cbs.dtu.dk/services/NetPhos/) was used to predict the phosphorylation sites. Prediction of sumoylation sites was performed by using GPS-SUMO software (http://sumosp.biocuckoo.org).

## Whole mount in situ hybridization (WMISH)

WMISH was performed as previously described by Russo (Russo et al. 2014) with some modifications. Hybridizations were carried out at 55 °C for 62 h using a mix of two antisense dygoxigenin (DIG)-labeled RNA probes of *Pl-Mitf*.

The first probe was 540 nt long (from amino acid 102 to amino acid 282) and the second was 438nt long (from amino acid 283 to amino acid 429), both covering most of the central region of *Pl-Mitf* cDNA. After extensive washing, embryos were incubated with an anti-DIG alkaline phosphatase-conjugated antibody (Roche Applied Science, Penzberg, Germany) for 2 h at room temperature. The DIG-labeled probes were detected by staining with the chromogenic 5-bromo-4-chloro-3-indolyl-phosphate (BCIP) and 4-toluidine/4-nitro blue tetrazolium chloride substrates (NBT) (Roche). Control hybridization reactions with sense probe did not show any specific signal. Images

**Table 1** Similarity percentages, respect to the number of overlapping amino acids, among Pl-Mitf and MITF protein sequences from other organisms, with relative Accession numbers and class/phylum of membership

| Species of organisms | Percentage of similarity/ number of amino acids | Accession numbers | Protein name | Class/Phylum |
|---|---|---|---|---|
| *Paracentrotus lividus* | | MK229196 | MITF | Echinoids/Echinoderms |
| *Strongylocentrotus purpuratus* | 94%/522 | XP_783071.3 | MITF-X1 | Echinoids/Echinoderms |
| *Strongylocentrotus purpuratus* | 94%/522 | XP_011682044.1 | MITF-X2 | Echinoids/Echinoderms |
| *Strongylocentrotus purpuratus* | 94%/522 | XP_011682045.1 | MITF-X3 | Echinoids/Echinoderms |
| *Acanthaster planci* | 71%/411 | XP_022108185.1 | MITF-X2 | Echinoids/Echinoderms |
| *Branchiostoma belcheri* | 70%/385 | XP_019634219.1 | MITF-X3 | Leptocardii/Chordates |
| *Salmo salar* | 63%/504 | XP_014002037.1 | MITF-X4 | Fishes/Chordates |
| *Danio rerio* | 65%/399 | XM_696860 | MITFA | Fishes/Chordates |
| *Gallus gallus* | 60%/525 | XP_015148453.2 | MITF-X2 | Birds/Chordates |
| *Xenopus laevis* | 64%/498 | NP_001165646 | MITF L homeolog | Amphibians/Chordates |
| *Homo sapiens* | 59%/526 | NP_937802.1 | MITF-X1 | Mammals/Chordates |
| *Drosophila melanogaster* | 54%/467 | NP_001033807.1 | MITF-B | Insects/Arthropods |
| *Caenorhabditis elegans* | 60%/289 | NP_001350991.1 | HLH protein | Chromadorea/Nematodes |

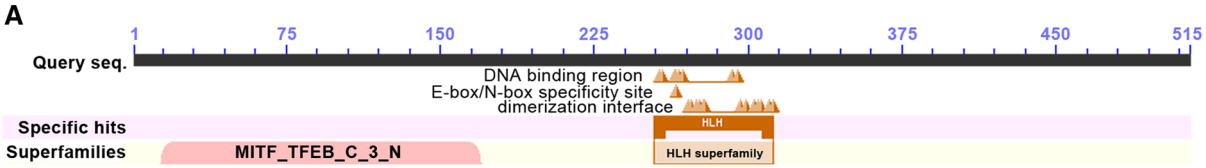
A
1
75
150
225
300
375
450
515
Query seq.
DNA binding region
E-box/N-box specificity site
dimerization interface
Specific hits
HLH
Superfamilies
MITF_TFEB_C_3_N
HLH superfamily

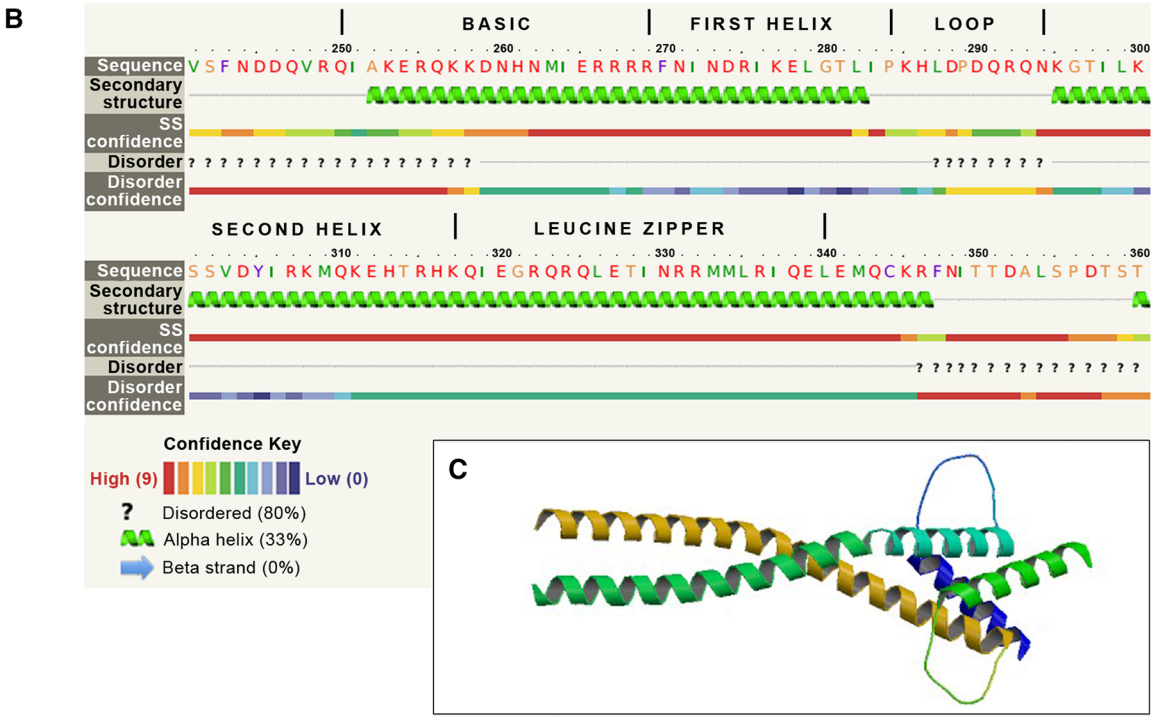
B
BASIC
FIRST HELIX
LOOP
Sequence
Secondary structure
SS confidence
Disorder
Disorder confidence
SECOND HELIX
LEUCINE ZIPPER
Confidence Key
High (9)
Low (0)
Disordered (80%)
Alpha helix (33%)
Beta strand (0%)
C

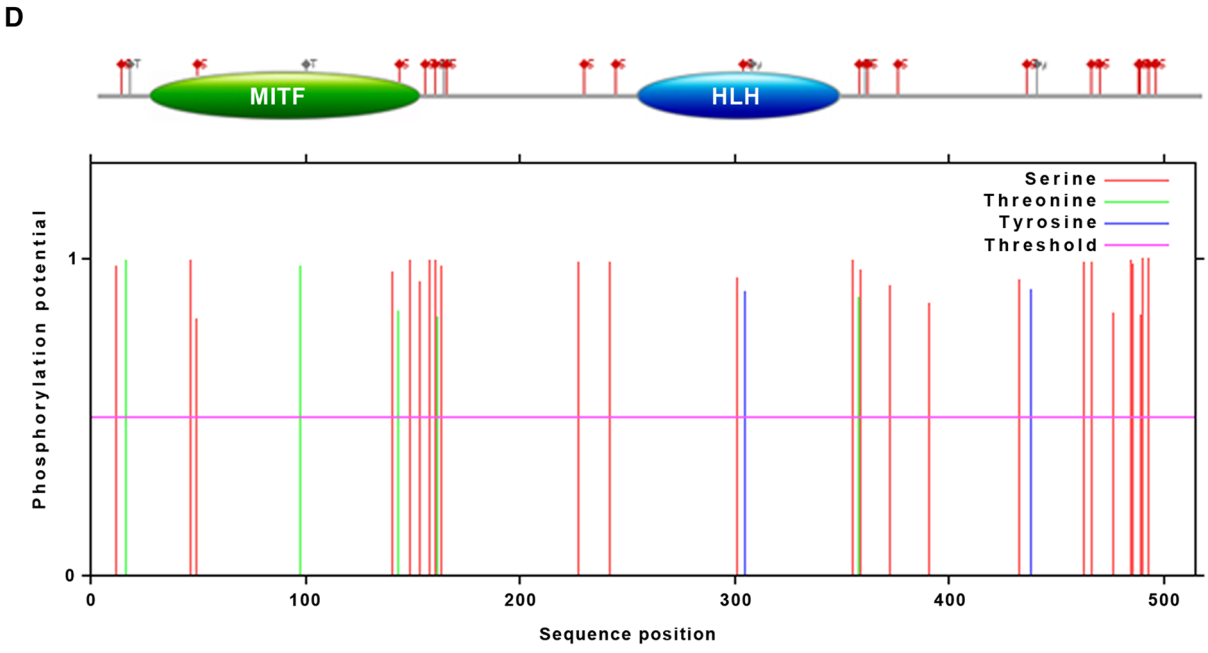
D
MITF
HLH
Serine
Threonine
Tyrosine
Threshold
Phosphorylation potential
Sequence position

◂**Fig. 1** Pl-Mitf protein analysis. **a** Diagram of Pl-Mitf protein by BLAST program, showing the most conserved and the specific regions of the superfamily. MITF_TFEB_C_3_N: MITF/TFEB/TFE3 superfamily; HLH: Helix–loop–helix domain; E-box/N-box specificity site: site of binding to E-box/N-box DNA consensus sequence. **b** Secondary structure of the DNA binding domain of Pl-Mitf transcription factor by Phyre2 program: the HLH domain is showed. **c** 3D structure of the Pl-Mitf protein DNA binding domain. **d** Scheme of the phosphorylation sites and their positions inside the Pl-Mitf protein, revealed by Netphos program with the score higher than 0.800. See online version for full color

were recorded with a digital camera mounted on a microscope Zeiss Axioscop 2 plus.

## Results

### Isolation of Pl-Mitf gene and in silico protein analysis

In this work, we isolated the cDNA corresponding to *Pl-Mitf* from late gastrula embryos. The amplification product contained the almost complete ORF, 1549 nt long, lacking only a few nucleotides (nt) at the 5′ end. For example, the isolated cDNA lacked 45 nt if compared to the *S. purpuratus Mitf*-X3 isoform, and 195 nt compared to the *Sp-Mitf*-X1 isoform. Table 1 reports the similarity percentages, respect to the number of overlapping amino acids, among Pl-Mitf and the MITF protein sequences from a number of organisms, obtained using the ALIGN software at ExPASy site. In particular, Pl-Mitf showed 94% of similarity with the three *S. purpuratus* MITF isoforms, including Sp-Mitf- X1 (XP_783071.3), Sp-Mitf-X2 (XP_011682044.1) and Sp-Mitf-X3 (XP_011682045.1), while it showed 71% of similarity with Mitf-X2 from the sea star *Acanthaster planci* (XP_022108185.1), 70% with the isoform X3 from the cephalochordate *Branchiostoma belcheri* (XP_019634219.1) and 63% with the isoform X4 from the fish *Salmo salar* (XP_014002037.1). In addition, the percentages of similarities with other organisms (the insect *D. melanogaster* and the mammalian *Homo sapiens*, the bird *Gallus gallus*, the amphibian *Xenopus laevis*) decreased, ranging from 64% with *X. laevis* to 54% with *D. melanogaster* (Table 1). As expected, the percentage of protein similarity was very high only with the cognate sea urchin, while it decreased in comparison with the sea star and the cephalochordate and decreased even more comparing Pl-Mitf protein with those of all the vertebrates.

The deduced Pl-Mitf protein was 515 aa long, with a theoretical pI 6.30 and an estimated molecular mass of 58.2 kDa. To predict the conserved structural domains that designate the MITF family of DNA-binding TFs, the deduced protein sequence of Pl-Mitf was blasted at GenBank NCBI (Fig. 1a). The predicted secondary structure of the bHLHzip DNA binding motif of Pl-Mitf was found by Phyre 2 software (Fig. 1b). The protein contains disordered regions with a percentage equal to 80%, alpha helices with a percentage of 33%, and no beta sheets. One functional domain was found located at the C-terminal half of the protein, ranging from 250 to 340 aa, including the basic domain (from 250 to 269 aa), the HLH domain, characterized by a first helix (270–284 aa), a loop (284–294 aa), and a second helix (295–317), and the leucine zipper domain (from 318 to 340 aa) (Fig. 1b). The Leucine rich region found in Pl-Mitf protein did not seem a canonical leucine zipper domain, which normally includes a series of Leucines (L) repeated every 7 aa, but showed an Isoleucine (I) as first amino acid (at the position 319), a L at 326, a Metionine (M) at 333 and a L at 341 (see the boxshade in Fig. S1). I and M are conservative substitutions being both hydrophobic/non polar (colored in red in the Clustal sequences alignment in Fig. S2).

The Figure S1 reports the "boxshade" protein sequences alignment of MITF proteins from diverse species of invertebrates (insects, echinoderms), cephalochordates and vertebrates (fishes, amphibians, birds, mammals), and displays, with black and grey boxes, the perfect identity of the amino acids, or the conserved substitutions, respectively. This alignment shows that the higher sequence homology concerned the region of the HLH domain (from 270 to 317), while other smaller regions of homology were scattered throughout the MITF proteins.

The model in Fig. 1c shows the simulation of a tertiary structure the *Pl-Mitf* DNA binding domain, based on the template of *Mus musculus* (4ATH, Mitf apo structure, Protein Data Bank, PDB software, https://www.rcsb.org). Figure S3 shows a movie of the most probable tertiary structure (with the highest score of 3.60) taken by the total Pl-Mitf protein, obtained with the I-Tasser software. In blue the N-terminal of the protein, and in red the C-terminal.

A further analysis of Pl-Mitf protein sequence has been performed by means of the Netphos program, an artificial network method that predicts phosphorylation sites, whose scores above 0.8 indicate positive predictions. According to the higher score obtained, many predicted phosphorylation sites were found in Pl-Mitf protein: 20 Serines (S), 5 Threonines (T) and only 2 Tyrosines (Y) (Fig. 1d). Then, we evaluated if these predicted sites were conserved among the invertebrates and vertebrates organisms here considered (in red in Fig. S1). This analysis has highlighted that only some of the 27 phosphorylation predicted sites were greatly conserved in both vertebrates and invertebrates, such as T98, T358, S153, S158, S355, S359, S485, S486, S489, S490, S493 and Y305. Other predicted phosphorylation sites have been conserved only within echinoderms or exclusively

among sea urchins, such as T162, S47, S141, S149, S163, S301, S373, S433, S463, S467, S490 and Y438.

The Pl-Mitf protein analysis by GPS-SUMO, a tool for the prediction of sumoylation sites and Sumo-interaction motifs, reported the presence of two sites of sumoylation at the positions K237 and K380, shown in Table 2. In Pl-Mitf, a site for SUMO protein interaction is present at the amino acid position 38–42 (Table 2).

## Phylogenetic analysis of MITF proteins

To construct the phylogenetic tree, we used Clustal O program to align Pl-MITF with the protein sequences from the organisms indicated in Table 1, including the sea urchin *S. purpuratus*, the sea star *A. planci*, the insect *D. melanogaster* and the nematode *C.elegans* as invertebrates, the lancelet *B. belcheri* as chordates and the mammalians *H. sapiens*, the bird *G. gallus*, the amphibian *X. laevis*, and fishes *S. salar* and *Danio rerio* as vertebrates (Fig. S2). The phylogenetic tree showed that Pl-Mitf clusters in the same clade with the sea urchin SpMitf-X1, X2 and X3 isoforms, confirming their major homology found by BLAST program. The sea urchins clusters together with the other echinoderm *A. planci*. All the vertebrate proteins form one distinct cluster also with *B. belcheri*, without including any of the invertebrate proteins analysed here. Furthermore, all vertebrates and invertebrates, subjected under natural evolution, share a common ancestor (Fig. 2).

## Temporal expression and spatial distribution of Pl-Mitf mRNA in *P. lividus* embryos during development

By real-time QPCR, we studied the temporal mRNA expression of *Pl-Mitf* at different developmental stages during sea urchin embryogenesis. The results are shown in Fig. 3 A. The levels of *Pl-Mitf* mRNA progressively decreased as the development of the embryo progressed after fertilization, namely eight cells (3 h post fertilization, hpf), morula (6 hpf) and blastula (18 hpf) stages, with values of 0.51, 0.2, 0.05

**Table 2** Pl-Mitf protein sumoylation and SUMO interactions sites

| Pl-Mitf | | | | |
|---|---|---|---|---|
| Position | Peptide | Score | Cut-off | Type |
| 38–42 | EKEDQQP VVVST SSSASAS | 62.154 | 59.29 | SUMO interaction |
| 237 | PTEIGKIKTEPVSFN | 49.492 | 16 | Sumoylation |
| 380 | SDIDFQVKVEPGTTH | 48.556 | 16 | Sumoylation |

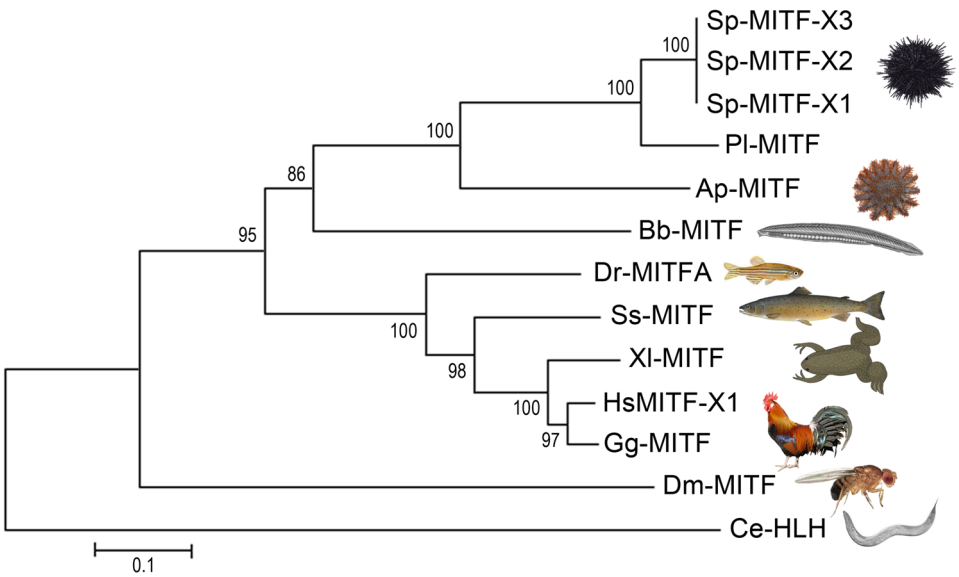


**Fig. 2** Evolutionary relationships of taxa for Pl-Mitf protein. Evolutionary analyses were conducted in MEGA6. The percentage of replicate trees in which the associated taxa clustered together in the bootstrap test (1000 replicates) are shown next to the branches. The tree is drawn to scale, with branch lengths in the same units as those of the evolutionary distances used to infer the phylogenetic tree. The evolutionary distances are in the units of the number of amino acid substitutions per site. All positions containing gaps and missing data were eliminated. Ap: *A. planci,* Bb: *B. belcheri*; Ce: *C. elegans;* Dm*: D. melanogaster;* Dr: *D. rerio;* Gg: *G. gallus*; Hs: *H. sapiens*; Pl: *P. lividus*; Sp*: S. purpuratus;* Ss: *Salmo salar*; Xl: *X. laevis*

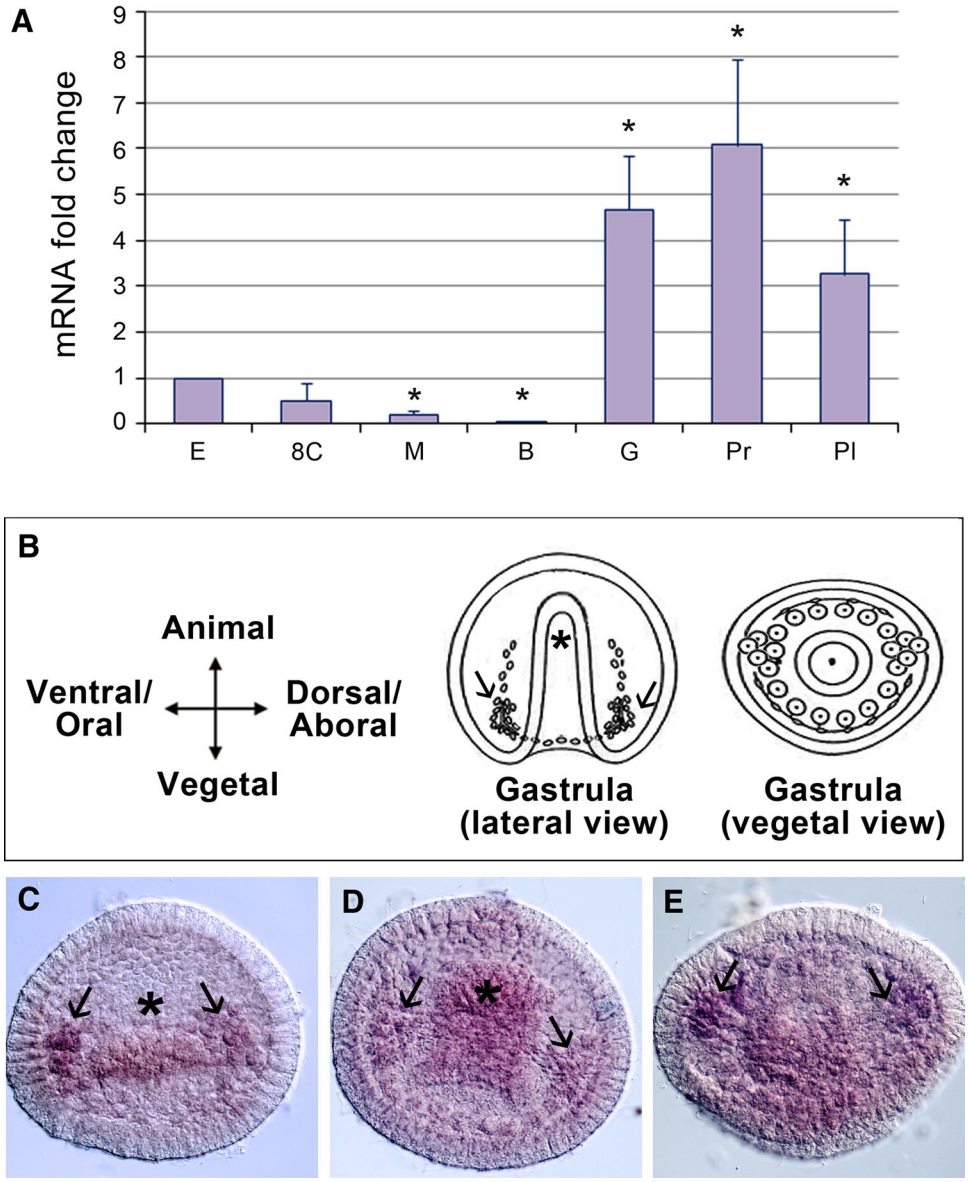


**Fig. 3** Temporal and spatial expression of *Pl-Mitf* transcripts. **a** Comparative QPCR analysis of *Pl-Mitf* transcription levels in *P. lividus* embryos. *Pl-Mitf* expression level throughout *P. lividus* sea urchin embryogenesis: E, unfertilized egg (used as reference sample and assumed as 1 in the histogram); 8C, 8 cells; M, morula; Bl, blastula; G, gastrula; Pr, prism; Pl, pluteus. The asterisk (*) indicates statistically significative variations to the relative reference sample. Each bar represents the mean of three independent experiments ± SD. **b–e** Spatial expression of *Pl-Mitf* during late sea urchin development. *Pl-Mitf* mRNA was studied by whole mount in situ hybridization. **b** Scheme of gastrula embryo, indicating the spatial orientation. **c** early gastrula (20hpf), lateral view; **d** late gastrula, lateral view; **e** late gastrula, vegetal view. Black arrows indicate primary mesenchyme cells. The asterisk (*) indicates the gut. See online version for full color

fold respectively, if normalized with the unfertilized egg, used as a control with an arbitrary value of 1. Interestingly, a noticeable *Pl-Mitf* mRNA increase (4.67 fold) was observed at the gastrula (24 hpf) stage, followed by a peak at prism stage (36hpf) (6.07 fold increase) and with a reduction of 50% at pluteus stage (48 hpf) (3.25 fold increase).

The spatial distribution of *Pl-Mitf* mRNA in sea urchin embryos was investigated by WMISH. Figure 3b shows a scheme of lateral and vegetal views of the sea urchin embryo at the late gastrula stage (24 hpf) with its orientation axes; the arrows indicate the PMCs, known to be the skeletogenic cells, while the asterisk indicates the archenteron, known to be the future gut. In blastula embryos at 18 hpf, *Pl-Mitf* seemed not to be expressed, in agreement with the very low expression levels recorded by QPCR analysis at this stage (data not shown). At the early (20hpf) and late (24hpf) gastrula stages, *Pl-Mitf* transcripts are expressed in the PMCs (Fig. 3c–e, black arrows), and in the developing archenteron (Fig. 3c–d, asterisks). At 48hpf, corresponding to the pluteus stage, the transcripts were hardly detectable by means of WMISH (not shown), although *Pl-Mitf* appeared expressed at this stage by QPCR analysis.

## In silico analysis of MITF protein interactions

In the attempt to elucidate what might be the function of MITF in the sea urchin embryo, we simulated a network showing all the predicted protein–protein relationships for MITF by using the STRING database and by comparing similar analyses obtained from different organisms. In

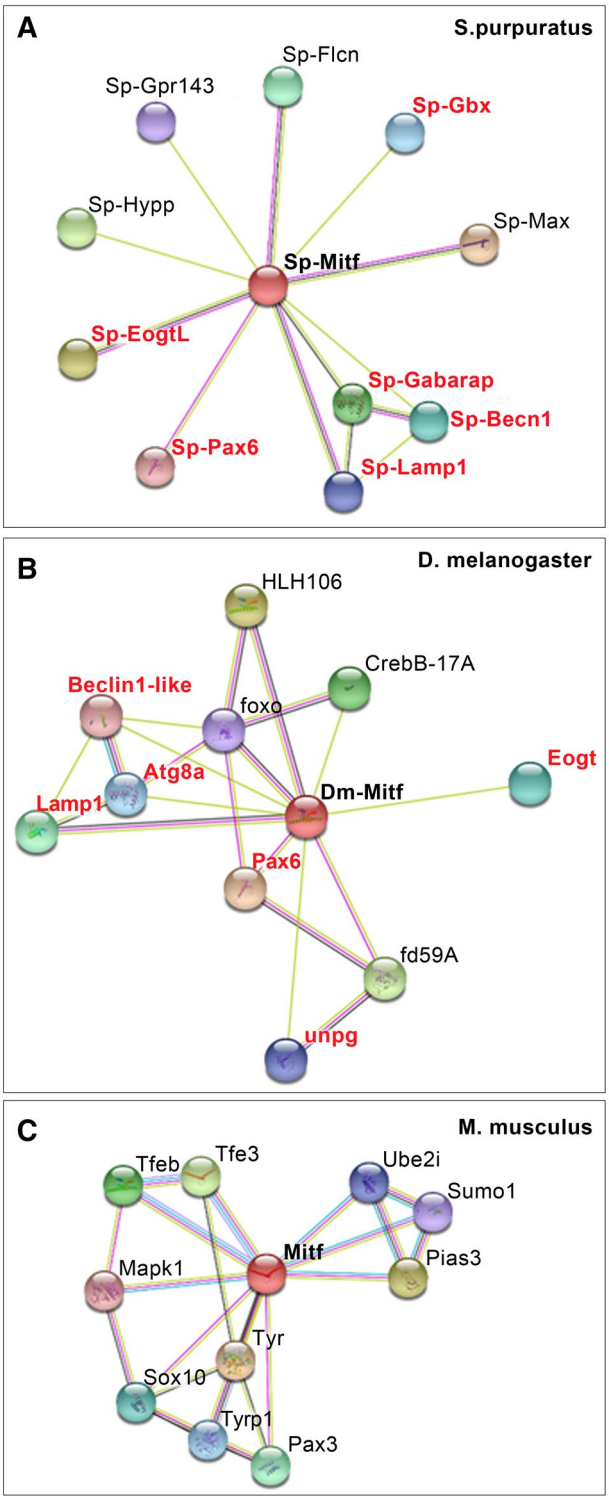


**Fig. 4** STRING in silico analysis of *S. purpuratus* (**a**), *D. melanogaster* (**b**) and *Mus musculus* (**c**) MITF interactive protein network. *S. purpuratus* proteins in red and bold are in common with *D. melanogaster*. See online version for full color

particular, since *P. lividus* genes are not annotated in the STRING database, we studied MITF protein associations in *S. purpuratus* (Fig. 4a), *D. melanogaster* (Fig. 4b) and *Mus musculus* (Fig. 4c). The analyses, performed with the default setting (medium confidence, 0.400), provided high scores of the predicted functional interactions, ranging from 0.574 to 0.999. The graphics reported in Fig. 4 are those created by the STRING software as well, with some manual modifications, particularly regarding *S. purpuratus*. The proteins associated with Sp-Mitf, as a result of the STRING analysis, are reported in the supplementary Table S1, in which some functions are also detailed. The sea urchin protein network showed that Sp-Mitf was associated with Gastrulation Brain homeobox (Sp-GBX), GABA type receptor-associated protein (Sp-Gabarap), Paired box 6 (Sp-Pax6), Lysosomal associated membrane protein (Sp-Lamp1), Sp-Becn1 (Beclin), Sp-EogtL. Interestingly, these proteins (red and bold in Fig. 4a) have also been found in the network of *Drosophila* (red and bold in Fig. 4b).

We found several differences between *S. purpuratus* and the mammalian. Differently from the invertebrate networks, mouse MITF protein interacts with the mitogen-activated protein kinases alias ERK (MAPK1), protein inhibitor of Stat6 (PIAS3), SRY-related HMG-box (Sox 10), Ubiquitin conjugating enzyme (Ube2i) and Small Ubiquitin Like Modifier 1 (Sumo1) proteins (Fig. 4c), all of them known to be also present in the *S. purpuratus* genome database (www.echinobase.org), but not present in Sp-Mitf STRING analysis (Fig. 4a).

## Discussion

In this study, we report the first evidence for the isolation of the cDNA encoding for MITF protein from *P. lividus* sea urchin embryo, referred to as *Pl-Mitf*. This protein shows high percentage of similarity with the three isoforms annotated in the *S. purpuratus* genome, and less homology with the *A. planci* sea star, with the cephalochordate *B.belcheri*, and with vertebrate organisms. The phylogenetic analysis indicated that the sea urchin MITF protein share a common ancestor with vertebrates and other invertebrates, suggesting that it is well conserved during the evolutionary pathway, and thus they might also share an analogous role.

In agreement with the evolutionary conservation of MITF proteins family throughout the animal kingdom, the sea urchin Pl-Mitf protein contains all the functional domains characteristic of the MITF family, i.e. the DNA binding bHLHzip domain. Although this last domain is highly conserved during evolution, in sea urchin MITF proteins only four out of five canonical L residues are present, and two of them are conservative substitutions, as I and M are both hydrophobic/non polar residues. Imperfect Leucine zipper

domains have been also shown in *D. melanogaster* (Hallsson and Benedikta 2007) and in other members of MYC family (Ferré-D'Amaré et al. 1993). Differently from other invertebrates, Mitf protein of the ascidia *Halocynthia roretzi* shows canonical leucines as vertebrates (Yajima et al. 2003). Therefore, the variable pattern of the bZip domain among different organisms suggests that MITF proteins might have undergone modular evolutive processes by "domain shuffling" (Jones 2004).

In addition, a conserved domain of transactivation (TAD) is located at the N-terminal of mammals MITF proteins, consisting of an IISLE core (ranging from the amino acids 230–234 in *H. sapiens*, see Fig. S1), which is partially conserved in Pl-Mitf protein (ranging from the amino acids 173–177) (Vachtenheim and Borovansky' 2010).

Analysis by Netphos software showed that Pl-Mitf protein contains some predicted phosphorylation sites that are conserved among all the vertebrates and invertebrates here analyzed, while other sites are exclusively conserved within echinoderms. It seems that the phosphorylation at these residues is important for the regulation of MITF functions in response to external stimuli. For example, the phosphorylation of MITF by AKT at the serine 510, as a response to EGF stimulation, affects its downstream targets, playing a crucial role in the melanogenesis and proliferation of melanocytes (Wang et al. 2016).

The temporal expression of *Pl-Mitf* mRNA in the sea urchin embryo revealed that the transcripts are already present in the unfertilized eggs, according to the well-known evidences about the maternal storage of large pools of mRNA and proteins in the cytoplasm, for later use throughout embryogenesis (Flytzanis et al. 1982).

The presence of *Pl-Mitf* mRNA in the PMCs and in the archenteron, as shown by WMISH experiments, is partially in agreement with what was found in the sea urchin *Lytechinus variegatus*. In particular, in addition to the PMCs, a small patch of *LvMitf*-expressing cells was observed at the tip of the archenteron, whose location suggests they might be a subset of the secondary mesenchyme cells (SMCs), i.e. the presumptive pigment cells, according to the known role of MITF protein in melanocytes (Levy et al. 2006) (see also Wu PhD thesis at https://dukespace.lib.duke.edu › dspace › bitstream). The pigment cells produce the Echinochrome A that is not involved in external pigmentation of the animals, but is important for innate immunity processes, having bactericidal activity (Service and Wardlaw 1985). Echinochrome A is absolutely different from mammalian melanin. Really, there is a single study reporting the attempt to isolate a melanin-like pigment from the black sea urchin *Diadema antillarum*, living in the Atlantic ocean. In *D. antillarum,* large epidermal chromatophores contain a black pigment that shows the characteristic properties of melanin (Millot and Jacobson 1951). In the following years other pigments, but not melanin-like, have been extracted from adult sea urchins, demonstrating essentially their antioxidant property (Powell et al. 2014).

In *P. lividus*, in addition to the presumptive SMCs, the entire archenteron is labeled with the Mitf probe, thus suggesting a further unknown role in the presumptive gut of the larval stage.

The localization of *Pl-Mitf* in the PMCs is somewhat unexpected, although interesting, since PMCs are devoted to forming only the larval skeleton. However, recent studies showed that MITF has also an important role in mammal osteoclastogenesis, cooperating with other TFs, such as NFATc1, PU.1, FOS and NF-kB, to induce osteoclast-specific genes, indicating a very high complexity in the transcriptional machinery during osteoclastogenesis (Asagiri and Takayanagi 2007; Lu et al. 2014). There are few peculiar characteristics of the PMCs that make them somewhat similar to osteoclasts, i.e. the involvement in the skeleton development, their migratory capability and the formation of multinucleated syncytia. Thus, MITF expression in the PMCs could be consistent with an unkown role in some stages of the sea urchin skeletogenesis. Other TFs have been isolated from *P.lividus*, such as the homologous of JUN and FOS-related antigen TFs, referred to as *Pl-jun* and *Pl-Fra,* whose mRNAs were both located in the PMCs, suggesting a potential role in skeletogenesis (Russo et al. 2014, 2018).

The STRING analysis allowed us to evaluate the relationships existing among MITF and other proteins in different organisms, including *S. purpuratus*, *D. melanogaster* and *M. musculus*. A number of proteins, such as MAPK1 (ERK2), PIAS3 (inhibitor of STAT proteins), TFEB (a TF associated with MITF) and SUMO1, were found to interact with mouse MITF, while they are not associated with *S. purpuratus* MITF, although some of these proteins are present in the Echinoderm genome datatabase.

For example, on the basis of the predicted sites for sumoylation found in *Pl-Mitf* sequence, we would have expected to find the SUMO protein in the sea urchin STRING analysis. SUMO are a family of small proteins, whose role is the post-translational modification of target proteins. It is known that sumoylation affects MITF transcriptional activity, and it depends on the number of multiple MITF binding sites in the promoter of target genes (Miller et al. 2005). The fact that SUMO, as well as other mouse proteins, is not present in the Sp-Mitf STRING analysis doesn't exclude a possible interaction between the two proteins in the sea urchin; it rather means that currently no evidence has been provided of a possible association between them, either from databases or from experimental research.

The STRING analysis has demonstrated that the proteins associated with Sp-Mitf are more similar to those of *D. melanogaster* than to those of the mouse, thus suggesting that sea urchin and insect MITF proteins could share

a similar function. The proteins found in the sea urchin STRING analysis, as well as in *D. melanogaster*, were Sp-GBX, Sp-Gabarap, Sp-Pax6, Sp-Lamp1, Sp-Becn, Sp-unpg, Sp-EogtL.

All these proteins play a role in different processes: in autophagy, such as Gabarap (Shpilka et al. 2011) and Beclin1 (Kang et al. 2011); in eye development, such as Pax6 corresponding to eyeless (ey) in *Drosophila* (Halder et al. 1995); in brain development, such as Unpg (Hirth et al. 2003) and Gbx (Waters and Lewandoski 2006). Although the sea urchin does not possess well-defined eyes, it has sense organs, capable of distinguishing the light. In echinoderms, light reception is due to the presence of different photoreceptors, including also non-pigmented dermal photoreceptors. One of the best studied examples of dermal photoreception was found in the sea urchin tube feets, in which rhabdomeric opsin and PAX6 genes are strongly expressed, highlighting their photoreceptor function (Zhao et al. 2014).

In conclusion, vertebrate MITF protein can regulate different biological processes such as osteogenesis, neurogenesis, cell proliferation and survival, oncogenesis, invasivaness, cell stress, and is considered the master regulator of melanocyte development. It contributes to hair and skin color. In the eye, MITF is specifically expressed in the retinal pigment epithelial cells, which are deputed to detect light and colors, while in the inner ear it plays an important role in hearing. It also regulates the development of osteoclasts and mast cells, that play a role in allergic reactions (Jones 2004; Levy et al. 2006). In freshwater fish, *Danio rerio*, the abrogation of MITF activity leads to melanoma regression and increased apoptosis (Lister et al. 2013).

While the role of MITF is quite clear and defined in vertebrates, and numerous mutations have been well studied over the past years, in invertebrates its role is still unclear. No MITF mutations have so far been identified in invertebrates, such as *C. elegans* (Rehli et al. 1999) and *D. melanogaster* (Hallsson and Benedikta 2007). However, while in *Drosophila* MITF protein might be involved in the eye development, in *C. elegans*, without pigment cells neither melanin production, it might have a different, and to date unknown, function. A very recent study describes the characterization of MITF in the mollusk *Patinopecten yessoensis*, where it seems involved in shell pigmentation (Mao et al. 2019).

Currently, there is no definite knowledge about the real functional role of MITF in invertebrates, such as the sea urchins, but our results provide the first evidence of the presence of *Pl-Mitf* in skeletogenesis cells and in the gut, suggesting a potential role during *P. lividus* sea urchin development.

**Acknowledgements** This research was supported by the Joint Research Project 2015–2017, as part of the Bilateral Agreement of Scientific and Technological Cooperation between the Consiglio Nazionale delle Ricerche of Italy (CNR) and the Russian Foundation for Basic Research (RFBR). We thank Mr Mauro Biondo and Alessandro Pensato for technical assistance.

**Author contributions** The conception and the design of the work was formulated by RR and FZ. Bioinformatics analyses were done by RR. The laboratory experiments were performed by RR, MC and FZ. The statistic analysis was carried out by MC. The analyses of experimental data and interpretation of data were done by RR, NL and FZ. The manuscript was written, validated and revised by RR, NL, MC and FZ.

## Compliance with ethical standards

**Conflict of interest** The authors declare that they have no conflict of interest.

## References

Asagiri M, Takayanagi H (2007) The molecular understanding of osteoclast differentiation. Bone 40:251–264. https://doi.org/10.1016/j.bone.2006.09.023

Bonaventura R, Zito F, Chiaramonte M et al (2018) Nickel toxicity in *P. lividus* embryos: dose dependent effects and gene expression analysis. Mar Environ Res 139:113–121. https://doi.org/10.1016/j.marenvres.2018.05.002

Chiaramonte M (2019) Evolutionary conserved pathway of the innate immune response after a viral insult in *Paracentrotus lividus* sea urchin. Int J Immunogenet. https://doi.org/10.1111/iji.12424

Costa C, Karakostis K, Zito F, Matranga V (2012) Phylogenetic analysis and expression patterns of p16 and p19 in *Paracentrotus lividus* embryos. Dev Genes Evol 222:245–251. https://doi.org/10.1007/s00427-012-0405-9

Ferré-D'Amaré AR, Prendergast GC, Ziff EB, Burley SK (1993) Recognition by Max of its cognate DNA through a dimeric b/HLH/Z domain. Nature 363:38–45. https://doi.org/10.1038/363038a0

Flytzanis CN, Brandhorst BP, Britten RJ, Davidson EH (1982) Developmental patterns of cytoplasmic transcript prevalence in sea urchin embryos. Dev Biol 91:27–35. https://doi.org/10.1016/0012-1606(82)90004-5

Halder G, Callaerts P, Gehring WJ (1995) Induction of ectopic eyes by targeted expression of the eyeless gene in Drosophila. Science 267:1788–1792. https://doi.org/10.1126/science.7892602

Hallsson H, Benedikta S (2007) Evolutionary sequence comparison of the Mitf gene reveals novel conserved domains. Pigment Cell Res. https://doi.org/10.1111/j.1600-0749.2007.00373.x

Hartman ML, Czyz M, Mitf ÁMÁ (2015) MITF in melanoma: mechanisms behind its expression and activity. Cell Mol Life Sci. https://doi.org/10.1007/s00018-014-1791-0

Hirth F, Kammermeier L, Frei E et al (2003) An urbilaterian origin of the tripartite brain: developmental genetic insights from Drosophila. Development. https://doi.org/10.1242/dev.00438

Hodgkinson CA, Moore KJ, Copeland NG, Jenkins NA (1993) Mutations at the mouse microphthalmia locus are associated with defects in a gene encoding a novel basic-helix-loop-helix-zipper protein. Cell 74:395–404

Howard-Ashby M, Materna SC, Brown CT et al (2006a) Gene families encoding transcription factors expressed in early development of *Strongylocentrotus purpuratus*. Dev Biol 300:90–107. https://doi.org/10.1016/j.ydbio.2006.08.033

Howard-Ashby M, Materna SC, Brown CT et al (2006b) Identification and characterization of homeobox transcription factor genes in *Strongylocentrotus purpuratus*, and their expression in embryonic

development. Dev Biol 300:74–89. https://doi.org/10.1016/j.ydbio.2006.08.039
Jones S (2004) An overview of the basic helix-loop-helix proteins. Genome Biol 5:1–6
Kang R, Zeh HJ, Lotze MT, Tang D (2011) The Beclin 1 network regulates autophagy and apoptosis. Cell Death Differ 18:571–580. https://doi.org/10.1038/cdd.2010.191
Katoh M, Katoh M (2004) Human FOX gene family (Review). Int J Oncol 25:1495–1500
Kelley LA, Sternberg MJE (2009) Protein structure prediction on the Web: a case study using the Phyre server. Nat Protoc 4:363–371. https://doi.org/10.1038/nprot.2009.2
Landschulz WH, Johnson PF, McKnight SL (1988) The leucine zipper: a hypothetical structure common to a new class of DNA binding proteins. Science 240:1759–1764. https://doi.org/10.1126/science.3289117
Levy C, Khaled M, Fisher DE (2006) MITF: master regulator of melanocyte development and melanoma oncogene. Trends Mol Med 12:406–414. https://doi.org/10.1016/j.molmed.2006.07.008
Lister JA, Capper A, Zeng Z et al (2013) A conditional zebrafish MITF mutation reveals MITF levels are critical for melanoma promotion vs regression in vivo. J Invest Dermatol 134:133–140. https://doi.org/10.1038/jid.2013.293
Livak KJ, Schmittgen TD (2001) Analysis of relative gene expression data using real-time quantitative PCR and the 2−ΔΔCT method. Methods 25:402–408. https://doi.org/10.1006/meth.2001.1262
Lu S, Li M, Lin Y (2010) Mitf induction by RANKL Is critical for osteoclastogenesis. Mol Biol Cell 21:1763–1771. https://doi.org/10.1091/mbc.E09
Lu SY, Li M, Lin YL (2014) Mitf regulates osteoclastogenesis by modulating NFATc1 activity. Exp Cell Res 328:32–43. https://doi.org/10.1016/j.yexcr.2014.08.018
Mao J, Zhang X, Zhang W et al (2019) Genome-wide identi fi cation, characterization and expression analysis of the MITF gene in Yesso scallops (*Patinopecten yessoensis*) with di ff erent shell colors. Gene 688:155–162. https://doi.org/10.1016/j.gene.2018.11.096
Materna SC, Berney K, Cameron RA (2006) The *S. purpuratus* genome: a comparative perspective. Dev Biol 300:485–495. https://doi.org/10.1016/j.ydbio.2006.09.033
Miller AJ, Levy C, Davis IJ et al (2005) Sumoylation of MITF and its related family members TFE3 and TFEB. J Biol Chem 280:146–155. https://doi.org/10.1074/jbc.M411757200
Millot N, Jacobson FW (1951) Phenolases in the Echinoid, *Diadema antillarum* Philippi. Nature 168:878. https://doi.org/10.1038/168878a0
Powell C, Hughes AD, Kelly MS et al (2014) LWT—food science and technology extraction and identification of antioxidant polyhydroxynaphthoquinone pigments from the sea urchin, *Psammechinus miliaris*. LWT Food Sci Technol 59:455–460. https://doi.org/10.1016/j.lwt.2014.05.016
Ragusa MA, Nicosia A, Costa S et al (2019) A survey on tubulin and arginine methyltransferase families sheds light on *P. lividus* embryo as model system for antiproliferative drug development. Int J Mol Sci 20:2136
Rehli M, Den Elzen N, Cassady AI et al (1999) Cloning and characterization of the Murine genes for bHLH-ZIP transcription factors TFEC and TFEB reveal a common gene organization for all MiT subfamily members. Genomics 120:111–120
Rizzo F, Fernandez-Serra M, Squarzoni P et al (2006) Identification and developmental expression of the ets gene family in the sea urchin (*Strongylocentrotus purpuratus*). Dev Biol 300:35–48. https://doi.org/10.1016/j.ydbio.2006.08.012
Roundy K, Smith R, Weis JJ, Weis JH (2003) Overexpression of RANKL implicates IFN-mediated elimination of B-cell precursors in the osteopetrotic bone of microphthalmic mice. J Bone Miner Res 18:280–288
Russo R, Pinsino A, Costa C et al (2014) The newly characterized Pl-jun is specifically expressed in skeletogenic cells of the *Paracentrotus lividus* sea urchin embryo. FEBS J 281:3828–3843. https://doi.org/10.1111/febs.12911
Russo R, Bonaventura R, Chiaramonte M et al (2018) Response to metals treatment of Fra1, a member of the AP-1 transcription factor family, in *P. lividus* sea urchin embryos. Mar Environ Res 139:99–112. https://doi.org/10.1016/j.marenvres.2018.05.003
Saitou N, Nei M (1987) The neighbor-joining method: a new method for reconstructing phylogenetic trees. Mol Biol Evol 4:406–425
Service M, Wardlaw AC (1985) Bactericidal activity of coelomic fluid of the sea urchin *Echinus Esculentus* on different marine bacteria. J Mar Biol Assoc UK 65:133–139. https://doi.org/10.1017/s0025315400060859
Shpilka T, Weidberg H, Pietrokovski S, Elazar Z (2011) Atg8: an autophagy-related ubiquitin-like protein family. Genome Biol 12:226
Slade L, Pulinilkunnil T (2017) The MiTF/TFE family of transcription factors: master regulators of organelle signaling, metabolism, and stress adaptation. Mol Cancer Res. https://doi.org/10.1158/1541-7786.MCR-17-0320
Sodergren E, Weinstock G, Davidson E, Al E (2006) The genome of the sea urchin *Strongylocentrotus purpuratus*. Science 314:941–952. https://doi.org/10.1126/science.1133609
Tamura K, Stecher G, Peterson D et al (2013) MEGA6: molecular evolutionary genetics analysis version 6.0. Mol Biol Evol 30:2725–2729. https://doi.org/10.1093/molbev/mst197
Tu Q, Brown CT, Davidson EH, Oliveri P (2006) Sea urchin Forkhead gene family: phylogeny and embryonic expression. Dev Biol 300:49–62. https://doi.org/10.1016/j.ydbio.2006.09.031
Vachtenheim J, Borovansky' J (2010) "Transcription physiology" of pigment formation in melanocytes: central role of MITF. Exp Dermatol. https://doi.org/10.1111/j.1600-0625.2009.01053.x
Wang C, Zhao L, Su Q et al (2016) The International Journal of Biochemistry Phosphorylation of MITF by AKT affects its downstream targets and causes TP53-dependent cell senescence. Int J Biochem Cell Biol 80:132–142. https://doi.org/10.1016/j.biocel.2016.09.029
Waters ST, Lewandoski M (2006) A threshold requirement for Gbx2 levels in hindbrain development. Development 2000:1991–2000. https://doi.org/10.1242/dev.02364
Widlund HR, Fisher DE (2003) Microphthalamia-associated transcription factor: a critical regulator of pigment cell development and survival. Oncogene. https://doi.org/10.1038/sj.onc.1206443
Yajima I, Endo K, Sato S et al (2003) Cloning and functional analysis of ascidian Mitf in vivo: insights into the origin of vertebrate pigment cells. Mech Dev 120:1489–1504. https://doi.org/10.1016/j.mod.2003.08.009
Zhao C, Ji N, Sun P et al (2014) Effects of light and covering behavior on PAX6 expression in the sea urchin *Strongylocentrotus intermedius*. PLoS ONE 9:1–6. https://doi.org/10.1371/journal.pone.0110895
Zuckerkandl E, Pauling L (1965) Evolutionary divergence and convergence in proteins. In: Bryson V, Vogel HJ (eds) Evolving genes and proteins. Academic Press, New York, pp 97–166